STUDY OF COUPLED DYNAMICS BETWEEN BODY AND LEGS OF A FOUR LEGGED WALKING ROBOT

V. L. Krishnan[(a)], P. M. Pathak[(b)], S. C. Jain[(c)]

Robotics and Control Laboratory
Mechanical and Industrial Engineering Department
Indian Institute of Technology, Roorkee, 247667, India

(a) vlk08dme@iitr.ernet.in, [(b)] pushpfme@iitr.ernet.in, [(c)] sjainfme@iitr.ernet.in

ABSTRACT
The paper presents a study of coupled dynamics between body and legs of a four legged robot with two articulate joints per leg. This study brings out the influence produced by the ground reaction forces through robot legs on the posture of robot body i.e. body rotations about *X*, *Y* and *Z* axis. An object oriented approach has been used for the bond graph modeling of locomotion dynamics of the four legged robot while taking into consideration the robot-ground interaction forces. Detailed kinematics analysis of a single leg has been carried out. Sub-model created for a single leg is repeatedly used for developing the bond graph model of the four legged walking robot. A multi bond graph is used to represent the system. A dynamical gait is proposed and implemented through joint control. Joint control has been achieved using a proportional derivative control law for each joint of the four legged robot. The robot locomotion has been successfully demonstrated through simulation and experiments on a robot prototype.

Keywords: Four legged walking robot, coupled dynamics between body and legs, bond graph modeling

1. INTRODUCTION

Legged robots have evolved as a better alternative compared to their wheeled counterparts for field applications such as military combat or transport operations, material handling and rescue operations, hazardous site inspection; and for extraterrestrial applications viz. Mars or space exploration etc. Legged robots are more suitable for such applications as they have greater agility and also they can move well on all kind of terrain whereas wheeled robots require only paved paths for better performance. Among the legged robots, six or more legged robots are suitable from the locomotion stability perspective. However, four legged robots offer a good compromise between locomotion stability and speed.

Research in rigid legged robots started almost in early 1980's with an attempt to realize rigid legged locomotion mainly on flat terrain. Waldron and McGhee (1986) presented the design of Adaptive Suspension Vehicle (ASV), which had morphology analogous to a six legged insect. Hartikainen et al. (1992) developed MECANT-I, a hexapod walking machine for forests applications. These robots mainly used statically stable gaits for their locomotion. Zhang and Song (1993) presented a study of the stability of generalized wave gaits. Gonzalez de Santos and Jimenez (1995) introduced discontinuous gaits and Estremera and Gonzalez de Santos (2002) proposed free gaits for locomotion of quadruped robots on irregular terrain. Later on researchers got motivated to explore dynamically stable gaits for realizing faster locomotion. Furusho et al. (1995) realized bounce gaits on SCAMPER, a rigid legged quadruped with its design similar to mammals. Estremera and Waldron (2006) proposed a leg thrust control method for the stabilization of dynamic gaits in rigid legged quadruped robot KOLT. Garcia et al. (2003) suggested that in addition to developing suitable gaits for legged locomotion, consideration of actuator dynamics and friction is essential for getting the real legged locomotion behaviour. Bowling (2005) examined the robot's ability to use ground contact to accelerate its body. Yoneda and Hirose (1992) employed biologically inspired approach to realize smooth transition from static to dynamic gait in the quadruped walking robot 'TITAN-IV'. Biological inspired approach refers to an extensive use of sensory feedback and reflex mechanisms (similar to that found in animals) for locomotion control. Further Kurazume et al. (2001) accomplished dynamic trot gait control for 'TITAN-VIII'. Inagaki et al. (2006) proposed a method for the gait generation and walking speed control of an autonomous decentralized multi-legged robot by using a wave Central Pattern Generator (CPG) model. Wyfells et al. (2010) has presented a design and realization of quadruped robot locomotion using Central pattern generators.

Legged robot is a multi-body dynamic system. Realization of various locomotion behaviors viz. walking, running etc. requires a precise understanding of the coupled dynamics between the body and legs of a legged robot. Also influence of ground reaction forces on the robot body is an important matter of

investigation because it is quite intuitive that instantaneous leg tip velocity of a legged robot depends upon the body state variables. Hence with the objective to investigate the coupled dynamics between the body and legs of a four legged walking robot, the present work has been carried out. This paper presents a three

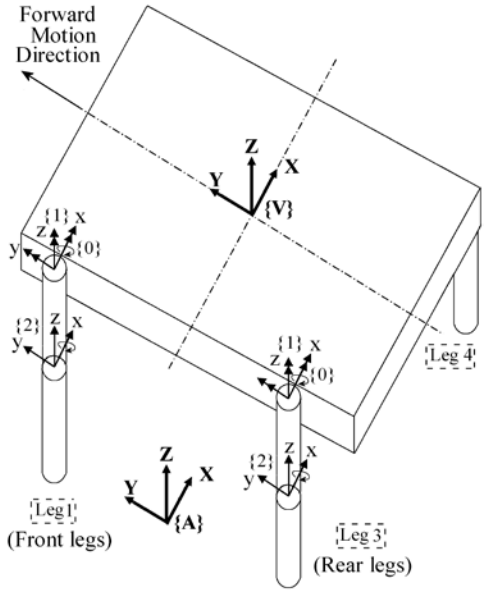

Figure 1: Schematic diagram of four legged robot

dimensional study of coupled dynamics between body and legs and generation of stable walking in a four legged robot. The coupled dynamics and robot locomotion has been demonstrated through simulation results and experiments on a robot prototype.

Bond graph technique (2006) has been used for object oriented modelling of the four legged robot. Bond graph is an explicit graphical tool for capturing the common energy structure of systems. It gives power exchange portray of a system. It provides a tool not only for the formulation of system equations, but also for intuition based discussion of system behavior viz. controllability, observability, fault diagnosis, etc. The language of bond graphs aspires to express general class physical systems through power interactions. The factors of power i.e., effort and flow, have different interpretations in different physical domains. Yet power can always be used as a generalized element to model coupled systems residing in different energy domains. In order to avoid repetitive modeling of same type of structure and to express a very large system in modular form, objects are created and then joined together to create an integrated system model. In the present work bond graph model of the four legged robot is created and simulated in SYMBOLS Shakti (2006), a bond graph modelling software.

2. BOND GRAPH MODELLING OF FOUR LEGGED ROBOT

Modelling of four legged robot consists of modelling of translational and angular dynamics of robot legs and body. Figure 1 shows the schematic diagram of a four legged robot model. In Fig. 1, $\{A\}$ is inertial frame of reference and $\{V\}$ is body frame. Each leg of the robot has two links. The joint between links i and i+1 is numbered as i+1. A coordinate frame $\{i+1\}$ is attached to (i+1) joint.

The linear dynamics of a body is governed by Euler's first law and angular dynamics by Euler's second law. Linear dynamics of a body can be given by

$$ {}^{A}F_{V} = M_{V}\ {}^{A}(\overset{A}{\dot{V}}_{G_V}) \qquad (1) $$

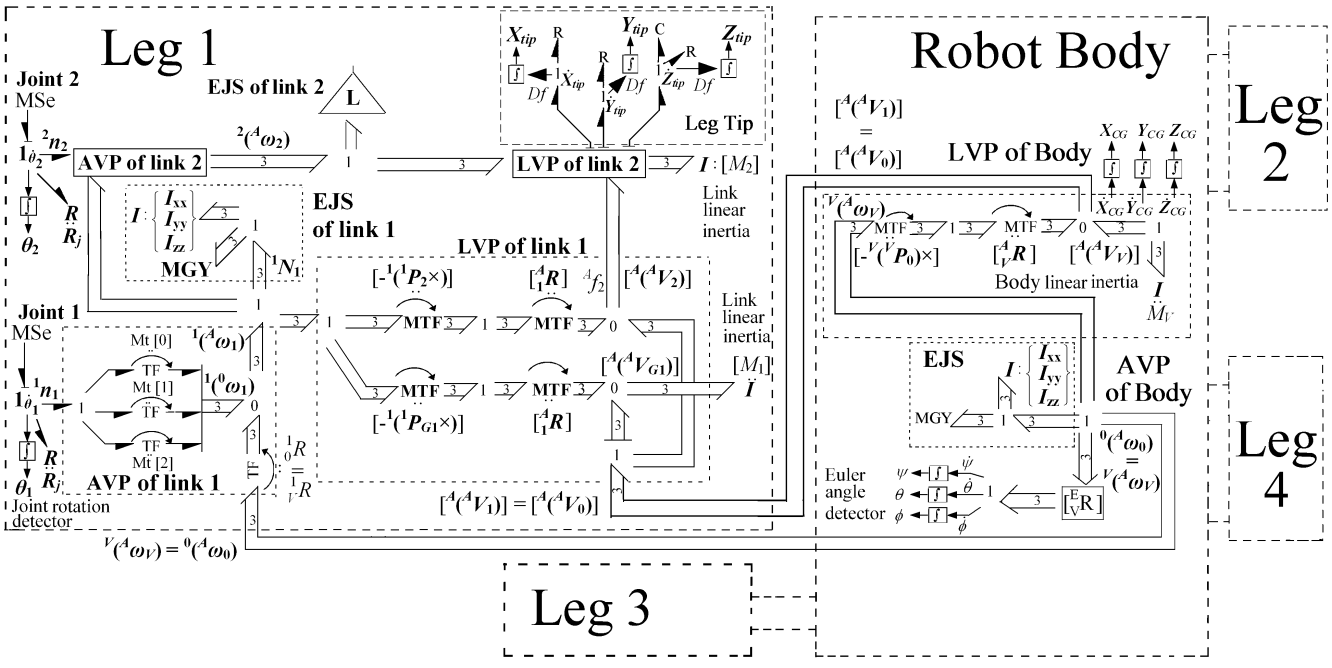

Figure 2: Multi bond graph of four legged robot

Where, ${}^{A}F_V$ is resultant of forces at joints ends and external forces acting at center of gravity (CG), expressed with respect to frame $\{A\}$; ${}^{A}(\overset{A}{\dot{V}}_{G_V})$ is acceleration of CG of body with respect to frame $\{A\}$; M_V is the mass of the body.

Angular dynamics of the body can be given by

$$ {}^{V}N_V = {}^{V}(\overset{A}{\dot{h}}_V) + {}^{V}({}^{A}\omega_V) \times {}^{V}({}^{A}h_V) \quad (2) $$

Where, ${}^{V}N_V$ is the moment acting on the body; ${}^{V}({}^{A}h_V)$ and ${}^{V}({}^{A}\omega_V)$ are respectively the angular momentum and angular velocity of body with reference to inertial reference frame $\{A\}$.

These fundamental equations of motion (1) and (2) along with linear velocity and angular velocity propagation relations for leg links (presented later in this section) guides the bond graph modeling of a four legged robot. Figure 2 shows the multi bond graph model of a four legged walking robot. The multi bond graph consists of sub model for the robot body and the four legs. Figure 3(a) and (b) respectively presents the bond graph of the 'LEG' and the 'Joint actuator' sub-models.

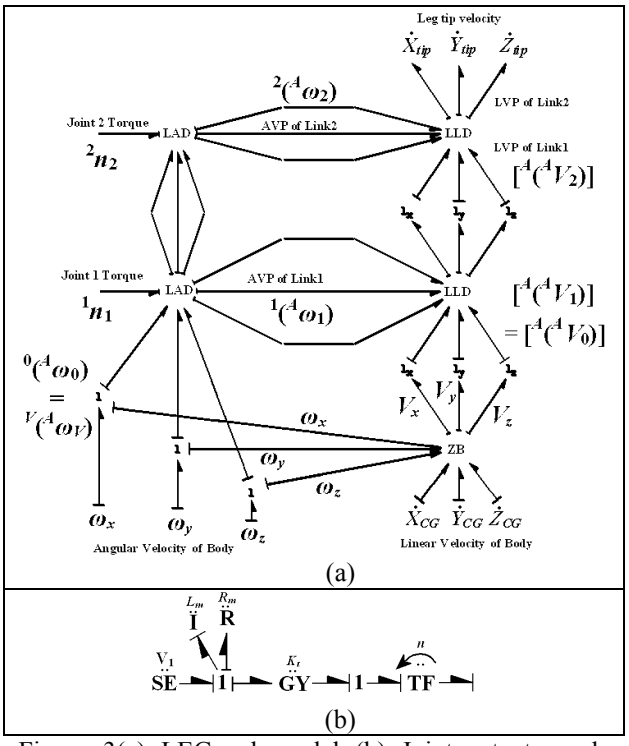

Figure 3(a) LEG sub-model (b) Joint actuator sub-model

Robot body sub model represents its translation and angular dynamics. The velocity of the body CG frame $\{V\}$ is obtained from the linear inertia of the body. Euler junction structure (EJS) can be used to represent the angular dynamics of a body (Mukherjee et al. 2006). Hence, it has been used to represent the rotational dynamics of the robot body as well as that of the links of robot legs in the present work.

The Euler equations used in the creation of the EJS sub-model of body are deduced from Eq. (2) and are given by Eq. (3) as

$$ N_x = I_x \dot{\omega}_x + (I_z - I_y)\omega_y \omega_z , \quad (3a) $$

$$ N_y = I_y \dot{\omega}_y + (I_x - I_z)\omega_z \omega_x , \quad (3b) $$

$$ N_z = I_z \dot{\omega}_z + (I_y - I_x)\omega_x \omega_y . \quad (3c) $$

Where N_x, N_y, N_z are the torques and $\dot{\omega}_x$, $\dot{\omega}_y$ and $\dot{\omega}_z$ are angular velocities acting about the principal axes of the corresponding body fixed frame. Linear velocity of the $\{0\}$ frame of each leg is given as

$$ {}^{A}({}^{A}V_0) = {}^{A}({}^{A}V_V) + {}^{A}_{V}R[-{}^{V}({}^{V}P_0) \times {}^{V}({}^{A}\omega_V)] \quad (4) $$

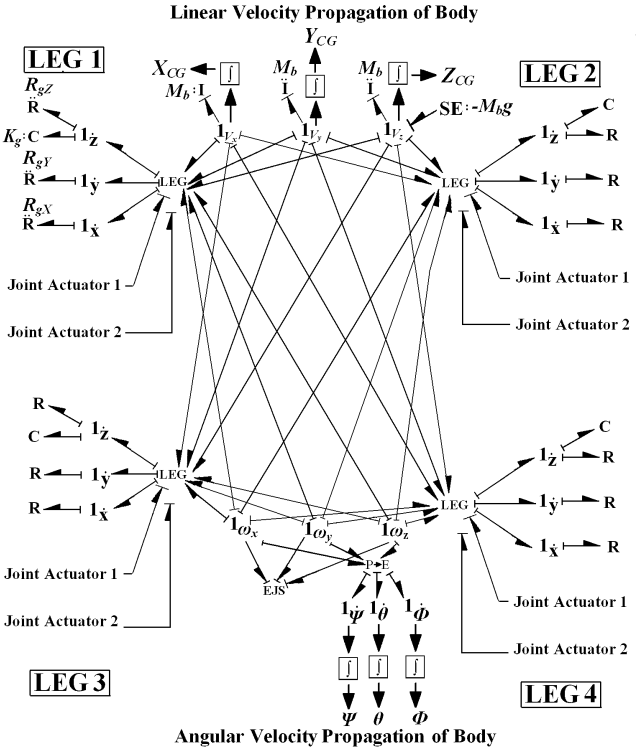

Figure 4: Bond graph of four legged robot locomotion dynamics

In Eq. 4, ${}^{A}_{V}R$ represent the transformation from body frame $\{V\}$ to inertial frame $\{A\}$ and can be expressed as,

$$ {}^{A}_{V}R = \begin{pmatrix} c\theta\, c\phi & s\psi\, s\theta\, c\phi - c\psi\, s\phi & c\psi\, s\theta\, c\phi + s\psi\, s\phi \\ c\theta\, s\phi & s\psi\, s\theta\, s\phi + c\psi\, c\phi & c\psi\, s\theta\, s\phi - s\psi\, c\phi \\ -s\theta & s\psi\, c\theta & c\psi\, c\theta \end{pmatrix} $$

ψ, θ and ϕ are the Euler angles representing robot body rotation about X, Y, Z axis of the body fixed frame $\{V\}$. ${}^{V}({}^{V}P_0)_i$ represent the position vector of frame $\{0\}$ of i^{th}

leg with respect to body CG frame {*V*}. It can be expressed as ${}^{V}({}^{V}P_0)_i = [R_{ix} \quad R_{iy} \quad R_{iz}]^T$, where *'i'* denotes leg 1 to 4. Value of R_{ix}, R_{iy} and R_{iz} corresponding to leg 1 to 4 is listed in Table 1 in appendix.

Linear Velocity Propagation (LVP) sub model shown in the 'Body' part of the multi bond graph in Fig. 2 takes the angular velocity from body ${}^{V}({}^{A}\omega_V)$ (obtained from EJS) and linear velocity ${}^{A}({}^{A}V_V)$ (decided by body mass) as input and gives out the velocity of {0} frame to the link 1 of each leg. Frame {0} and {1} are coincident for each leg. Hence, the velocity of frame {1} is same as frame {0} i.e. ${}^{A}({}^{A}V_1) = {}^{A}({}^{A}V_0)$.

'Leg' sub model, shown in detail in Fig. 3(a), represents a two DOF leg. 'Leg' takes angular and linear velocity of body and joint torques about *X*-axis as input. 'LEG' sub model uses Angular Velocity Propagation (AVP) and LVP sub models of links 1 and 2 and gives out leg tip velocity as output. Link lengths l_1 and l_2 are taken along the principal *Y*-axis of the links and hence represented in vector form as,

${}^{0}P_1 = [0 \quad 0 \quad 0]^T$, ${}^{1}P_2 = [0 \quad l_1 \quad 0]^T$, ${}^{2}P_3 = [0 \quad l_2 \quad 0]^T$. Thus 'LEG' furnishes complete dynamics of a two link leg. The various sub models shown in Fig. 2 for leg '1' can also be used to model leg 2, 3 and 4.

LVP and AVP sub models for leg links can be used to find the velocity of tip of link1 and link 2 of a leg i.e. frame {2} and frame {3} respectively. Governing equation for AVP of links of a leg can be given as per theory (Craig 2006),

$$ {}^{i+1}({}^{A}\omega_{i+1}) = {}^{i+1}_{i}\boldsymbol{R}\,{}^{i}({}^{A}\omega_i) + {}^{i+1}({}^{i}\omega_{i+1}) \qquad (5) $$

Where, ${}^{i+1}({}^{i}\omega_{i+1})$ is the angular velocity of (i+1) link as observed from i^{th} link and expressed in (i+1)th frame. The term can be expressed for link 1 and 2 respectively as,

${}^{1}({}^{0}\omega_1) = [\dot{\theta}_1 \quad 0 \quad 0]^T$, ${}^{2}({}^{1}\omega_2) = [\dot{\theta}_2 \quad 0 \quad 0]^T$.

${}^{i}({}^{A}\omega_i)$ is the angular velocity of the i^{th} link with respect to inertial frame {*A*} and expressed in i^{th} frame. ${}^{i+1}({}^{A}\omega_{i+1})$ is the angular velocity of (i+1) link with respect to inertial frame and expressed in (i+1)th frame. The above equation (5) is represented by the sub model 'AVP of Link' in each leg of the robot.

Governing equation for the link tip velocity and link CG velocity are given as,

$$ {}^{A}({}^{A}V_{i+1}) = {}^{A}({}^{A}V_i) + {}^{A}_{i}R[{}^{i}({}^{A}\omega_i) \times {}^{i}({}^{i}P_{i+1})] \qquad (6) $$

This can be simplified as,

$$ [{}^{A}({}^{A}V_{i+1})] = [{}^{A}({}^{A}V_i)] + [{}^{A}_{i}R][-{}^{i}({}^{i}P_{i+1}\times)][{}^{i}({}^{A}\omega_i)] \qquad (7) $$

For position of a link CG, ${}^{i}({}^{i}P_{G_i}) = [0 \; l_{Gi} \; 0]^T$

$$ [{}^{A}({}^{A}V_{G_i})] = [{}^{A}({}^{A}V_i)] + [{}^{A}_{i}R][-{}^{i}({}^{i}P_{G_i}\times)][{}^{i}({}^{A}\omega_i)] \qquad (8) $$

Equations (6), (7), (8) represent the LVP of Link in each leg of the robot. CG velocity of links depends on link inertia. In bond graph model '*I*' elements (representing mass of a link), are attached at flow junctions. They yield the CG velocities of links. The starting point of the current link is same as the previous link tip. Hence, the tip velocity of the previous link and the angular velocity of the current link are used to find the tip velocity and CG velocity of the current link. ${}^{i}({}^{A}\omega_i)$ in above equations can be obtained from the AVP for the current link.

The leg tip sub-model in Fig. 2 represents the modelling of leg tip-ground interaction. The robot is assumed to be walking on a hard surface with no slipping of legs. An 'R' element is appended to '1' junction of each leg in the *X* and *Y* direction, to model the frictional resistance offered by ground. Similarly, 'C' and 'R' elements are attached in *Z*-direction to model the normal reaction force from the ground. Leg tip position detectors in each direction yields the leg tip position coordinates.

The integrated bond graph model representing the four legged robot locomotion dynamics is presented in Fig. 4. Parametric values assumed for the purpose of simulation of the four legged robot model are shown in Table 2 in appendix.

3. GAIT PATTERN

Gait pattern represents the sequence of leg movements required for realizing locomotion of a robot while maintaining body stability. In the present work, a bounding walk gait pattern has been implemented for achieving robot locomotion. The gait has been used by Lasa and Buehler (2000) for their single-link legged quadruped robot SCOUT-II. In this gait pattern, either the front or rear legs of the quadruped robot are simultaneously lifted up or brought down to the ground in a particular phase of the gait. Figure 5(i-viii) represents schematically the eight phases of the gait pattern of a locomotion cycle.

To implement the gait pattern, position of the joints of each leg must be controllable. The voltage supplied for controlling the position of joints can be given as

$$ V_i = K_P\left(\theta_{di} - \theta_i\right) + K_V\left(\dot{\theta}_{di} - \dot{\theta}_i\right) \qquad (9) $$

Where, V_i is the input voltage supplied at the i^{th} joint of a leg. The voltage supply to a joint actuator is implemented in bond graph, through an '*SE*' element of joint actuator sub-model shown in Fig. 3(b). K_P and K_V are respectively the proportional and derivative gains; θ_{di} is the desired value of rotation, θ_i is the actual value of rotation, $\dot{\theta}_{di}$ is the desired joint velocity and $\dot{\theta}_i$ is the actual joint velocity.

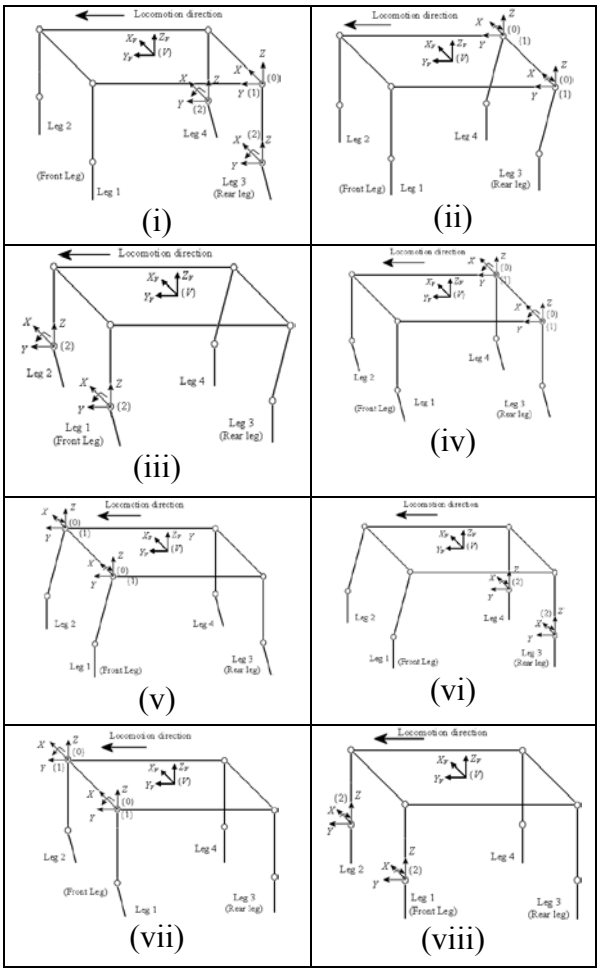

Figure 5: Phases of gait pattern

The joint reference command used for moving a particular joint to the desired position 'θ_{i+1}' at the end of a certain time interval Δt_{i+1} i.e. (t_{i+1}-t_i), can be expressed by the following equation,

$$\theta_{i+1} = \theta_i \pm k(1 - e^{-\lambda(t_{i+1} - t_i)}) \qquad (10)$$

In Eq. (14), θ_i and θ_{i+1} respectively represents the joint angular displacement values at the beginning and end of a time interval Δt_{i+1}; k is a factor by which the joint angle is to be increased or decreased, λ is an integer. It can be noted from Eq. (14) if $t = t_i$, then $\theta = \theta_i$ and when $t = t_{i+1}$ then $\theta = \theta_i \pm k$, for very large values of λ which leads the exponential term to a zero value.

4. SIMULATION RESULTS AND DISCUSSION

For the selected gait pattern and robot parameters, simulation has been carried out for 3 cycles. A locomotion cycle takes 3.2 seconds. Simulation results are presented in Fig. 6, 7, 8 and 9. Fig. 6(a) and (b) respectively shows front leg joint 1 displacement (θ_{1F}) and front leg joint 2 displacements (θ_{2F}) versus time. Similarly, rear leg joint 1 (θ_{1R}) and rear leg joint 2 (θ_{2R}) displacement versus time is presented in Fig. 7(a) and (b). It can be noted that the leg joint angular displacement plots corresponds with the specified gait pattern.

Figure 8(a), (b) and (c) respectively presents the variation of robot body Euler angles ψ, θ and ϕ versus time. ψ, θ and ϕ represents the robot body rotation about X, Y and Z axis. As a consequence of the selected gait

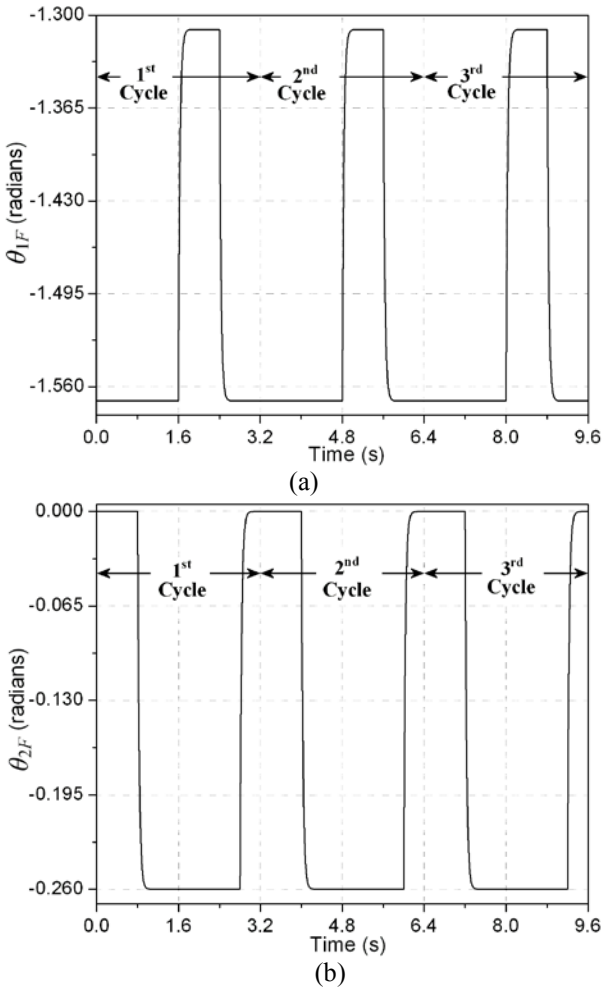

Figure 6: Simulation results of rigid legged quadruped robot locomotion: Front leg joint angular displacements (a) θ_{1F} (radians) versus time (s) (b) θ_{2F} (radians) versus time (s)

pattern for locomotion (in which the two front or rear legs are simultaneously lifted or brought down simultaneously), the body angular displacement 'ψ' is oscillatory, as shown in Fig. 8(a). Variation of 'ψ' with respect to time signifies the coupled dynamics between the legs and the body. In the figure, second cycle of locomotion has been further split into eight phases (of the specified gait pattern) to explain the coupled dynamics. It can be noted that a correspondence between the various phases of the gait pattern and the body pitching motion 'ψ' exists. For instance, in the first two phases of the gait pattern (i.e. Fig. 5(i) and (ii)) the rear leg links rotation should result in body pitching about +X-axis. The reason being the rear leg hip joint will be at lesser height as compared to its front leg

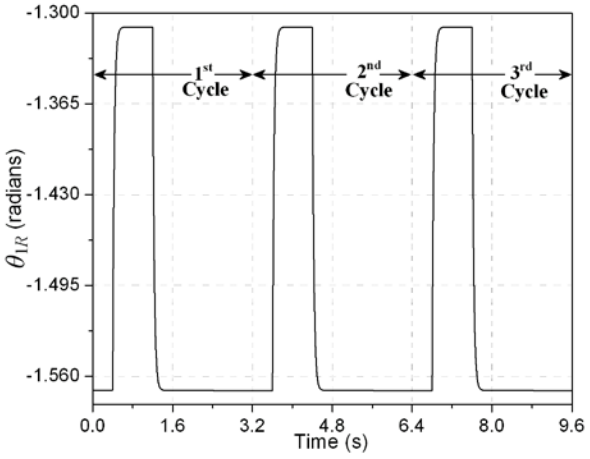

(a)

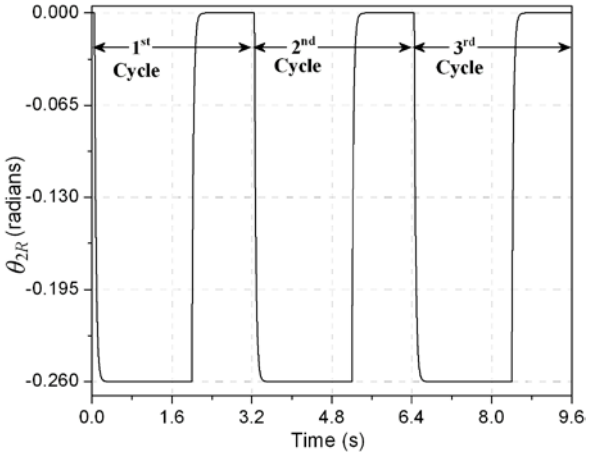

(b)

Figure 7: Simulation results of rigid legged quadruped robot locomotion: Rear leg joint angular displacements (a) θ_{1R} (radians) versus time (s) (b) θ_{2R} (radians) versus time (s)

counterpart due to the specified rotation. Simulation result in Fig. 8(a) validates this observation. Similarly corresponding to the gait pattern phase shown in Fig. 5(iv), pitching about *X* axis varies from positive to negative values due to the variation of the difference in the vertical height of front and rear leg hip joints. Similarly it can be observed that 'ψ' is almost equal to zero radians i.e. robot body is absolutely horizontal, at the beginning of a locomotion cycle, at the end of the fourth and eighth phase of a locomotion cycle. The reason for the fact is that the front and rear leg hip joints in the respective phases are at almost equal elevation.

Figure 8(b) indicates that there is no significant angular displacement 'θ' about *Y*-axis (as expected), because the joint torque is supplied only about *X*-axis. Figure 8(c) shows that the body is turning about +Z-axis. Figure 8(d) indicates quadruped robot progression, as since the robot body *CG* displacement occurs along positive *Y*-axis i.e. the direction of locomotion.

Figure 9(a), (b), (c) and (d) respectively shows the displacement of tip of legs 1, 2, 3 and 4, along positive *Y*-axis. It can be noted from the simulation results that the leg tip displacement values for leg 2 and 4 are greater than that of leg 1 and leg 3. Thus the simulation

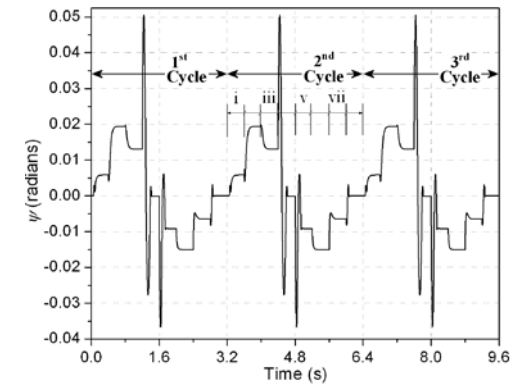

(a)

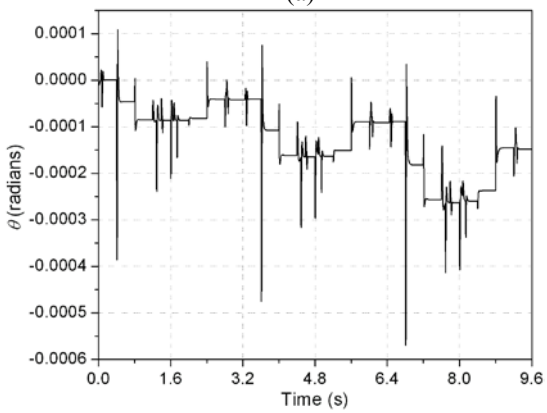

(b)

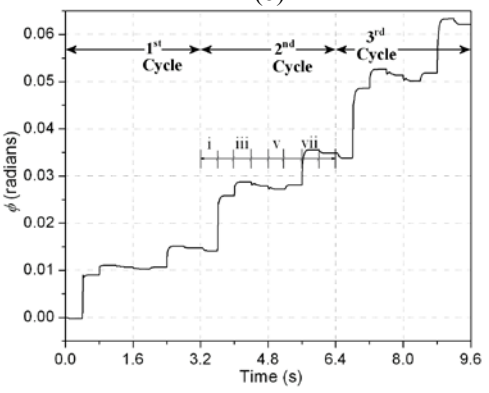

(c)

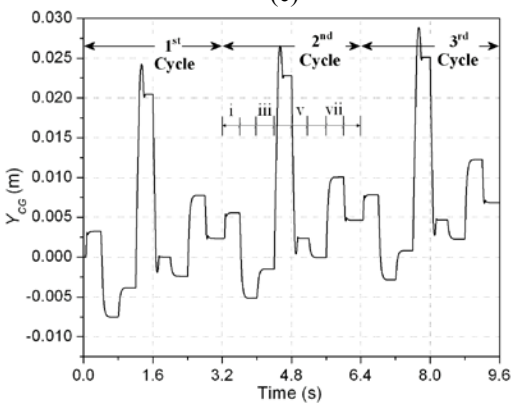

(d)

Figure 8: Simulation results of rigid legged quadruped robot locomotion (a) ψ (radians) versus time (s) (b) θ (radians) versus time (s) (c) ϕ (radians) versus time (s) (d) Y_{CG} (m) versus time (s)

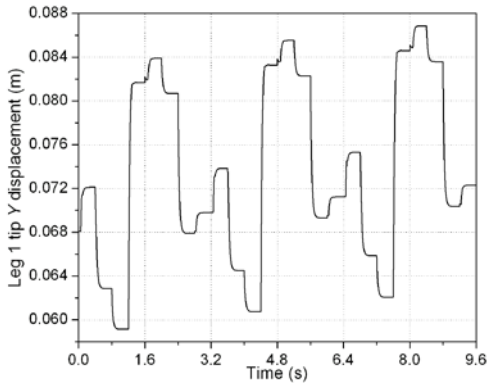

(a)

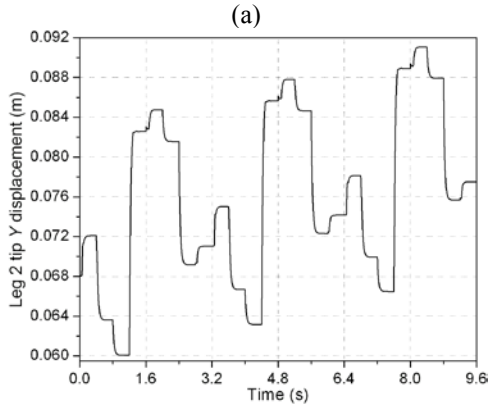

(b)

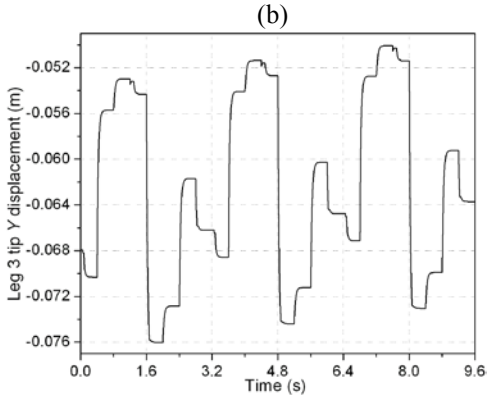

(c)

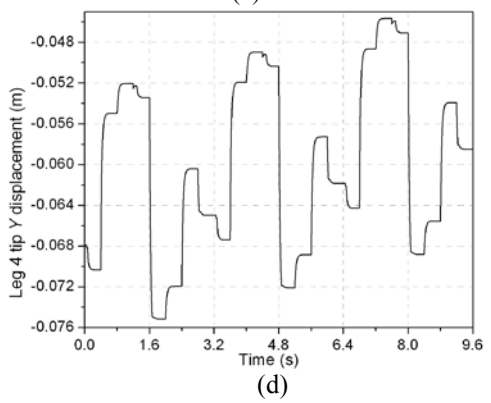

(d)

Figure 9: Simulation results of rigid legged quadruped robot locomotion: (a) Leg 1 tip *Y* displacement (m) versus time (s) (b) Leg 2 tip *Y* displacement (m) versus time (s) (c) Leg 3 tip *Y* displacement (m) versus time (s) (d) Leg 4 tip *Y* displacement (m) versus time (s)

results indicate that the robot is turning about positive *Z*-axis. The turning about *Z*-axis can be attributed to the modelling of leg tip-ground interaction.

The frictional resistance offered by the ground to legged robot locomotion has been modeled, by appending a dissipative R-element (bond graph element) at the 1-junction representing leg tip velocity. The value of the parameter '*R*' representing frictional resistance has been assigned greater value in *X*-direction compared to that in the locomotion direction i.e. $R_{gX} > R_{gY}$.

In the next section, the experimental realization of locomotion of quadruped robot prototype is presented.

5. EXPERIMENTAL RESULTS

Experimental set-up designed for realizing robot locomotion is presented in Fig. 10. The quadruped robot comprises of four legs and a body over which the controller CM5+ is mounted. The front and rear legs have been designed identical in all respects. Each leg of the quadruped robot has two rigid links connected through revolute joints, one at the hip and second one at the knee of a leg. The links are rotated through 'Dynamixel' series AX-12+ actuators, deployed at the joints.

Bioloid control behavior interface of the Robotis Inc. is used for the purpose of controlling robot locomotion. Control algorithm is fed to the CM5+ controller through a personal computer. A serial to USB data cable is used for the communication between the PC and the CM5+ controller. SMPS is used for supplying required power to the actuators and electronic circuitry. CM5+ controller uses ATMega 128 (128Kbyte flash memory) as the main processor in it. It operates in the voltage range of 7V-12V.

A program corresponding to the specified gait pattern is communicated to the controller CM5+. Consequently the robot locomotion is accomplished. Figure 11 presents the snapshots of locomotion of the quadruped robot. Snapshots indicate a clear progression of the robot. Figure 12 presents the leg tip and body CG

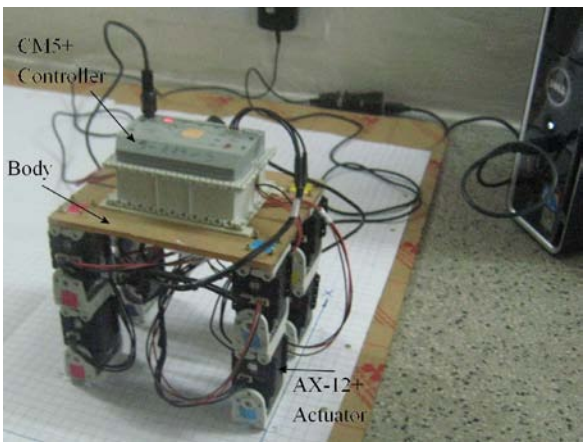

Figure 10: Experimental prototype of four legged robot

trajectory in *XY* plane, plotted using the experimental data. The body CG trajectory and the leg tip

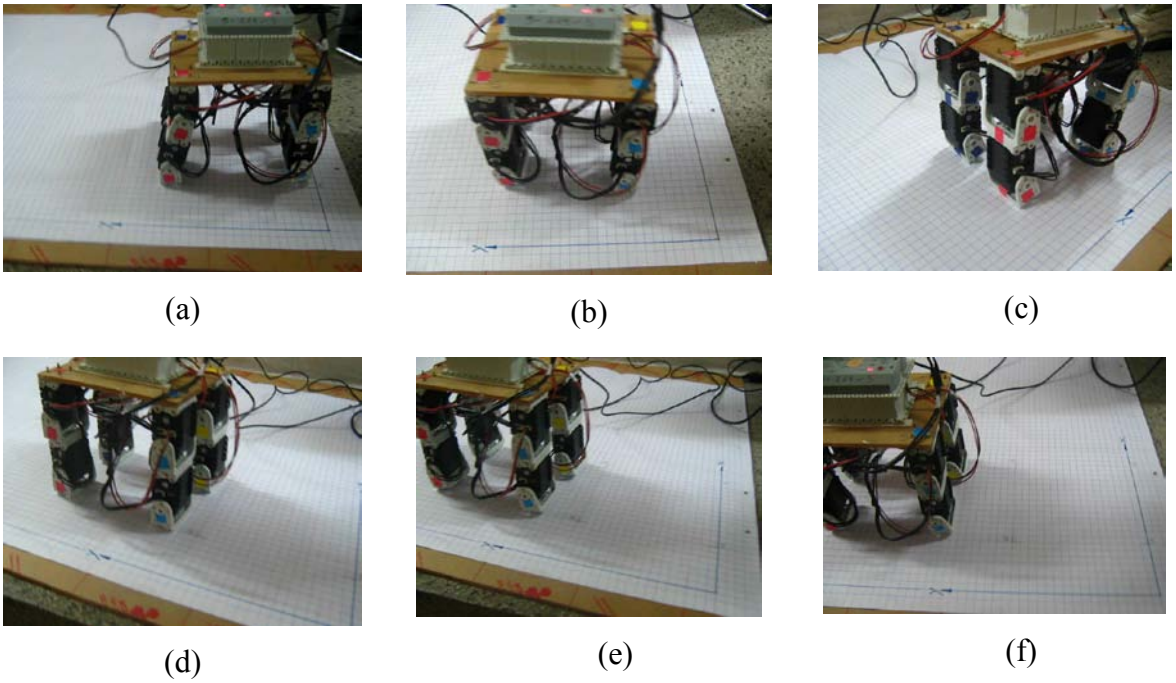

Figure 11: Snapshots of rigid legged quadruped robot locomotion

displacement plots indicate that the robot is almost progressing as desired, along a straight line in the locomotion direction. Slight deviation of the body CG and leg tip trajectories from the straight line path can be attributed to the unpredictable and arbitrary lag in command signals to the front or rear leg joint actuators.

Figure 13(a), (b), (c) and (d) respectively presents the actual and commanded joint angle displacement trajectories of joint 1 and 2 of the front and rear legs. There is a slight deviation in the commanded and actual joint trajectory along with some arbitrary lag in the front and rear joint trajectory.

6. CONCLUSIONS

The paper presents the coupled dynamics between the legs and body during locomotion. This study has been carried out through simulation as well as experiment on a four legged robot design with two articulate joints per leg. Modeling and simulation of the four legged robot has been carried out using bond graph technique. For the specified gait pattern, the body angular displacement trajectory for ψ and θ demonstrates the influence of ground reaction forces, transmitted through legs, on the robot body. The gait pattern has been tested on a quadruped robot experimental model and locomotion has been successfully realized.

This dynamic model of the four legged robot locomotion can be further extended for simulating running behavior, obstacle avoidance etc. Flexible leg concept may be incorporated to enable the robot to walk on uneven terrain. In fact the motivation for this work originated with a desire to build a model of four legged walking robot with flexible legs. Flexible legged robot model can be used to study the effect of flexible leg dynamics on the stability and impact tolerance of the robot.

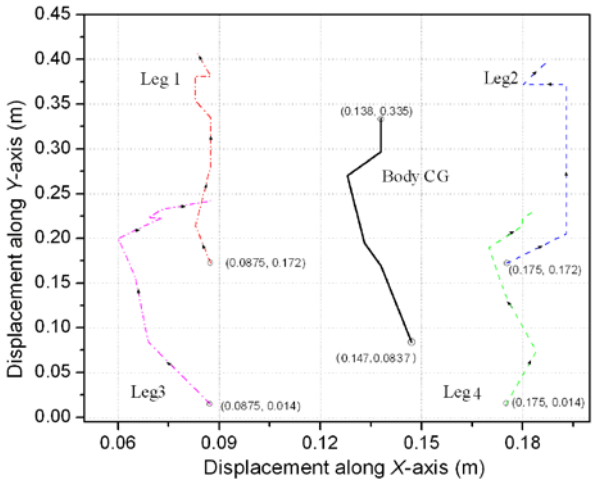

Figure 12: Experimental results of rigid legged quadruped robot locomotion: Leg tip and body CG displacement along *X*-axis (m) versus *Y*-axis (m)

APPENDIX

Table 1:Position of Frame {0} with respect to Body CG

Leg *'i'*	R_{ix}	R_{iy}	R_{iz}
Leg 1	-0.042	0.068	-0.045
Leg 2	0.042	0.068	-0.045
Leg 3	-0.042	-0.068	-0.045
Leg 4	0.042	-0.068	-0.045

Table 2: Four Legged Robot Parameters

Parameters	Value
Robot body mass	M_b = 0.43Kg;
Moment of Inertia (M. I.) of body	I_{BXX} = 0.007Kg-m^2, I_{BYY} = 0.004Kg-m^2, I_{BZZ} = 0.002Kg-m^2
Leg link lengths	l_1 = 0.068m, l_2 = 0.025m
Leg link mass	M_{l1}= 0.075Kg; M_{l2}= 0.015Kg
M. I. of link '1'	I_{xx1} = 0.0002Kg-m^2, I_{yy1} = 0.00025Kg-m^2, I_{zz1}= 0.00001Kg-m^2
M. I. of link '2'	I_{xx2} = 0.00001Kg-m^2, I_{yy2} = 0.000003Kg-m^2, I_{zz2}= 0.000004Kg-m^2
Joint actuator parameters	Inductance: L_m =0.001H; Resistance: R_m= 0.1Ohms; Motor constant: K_t = 0.2 N-m/A; Gear ratio: n = 254
Leg tip-ground interaction	Stiffness: K_g = 100000N/m; Damping: R_{gZ} = 1000N-s/m; Frictional resistance: R_{gX} = 800N-s/m, R_{gY} = 400N-s/m
Gain Values	Proportional gain: K_P = 2500V/rad; Derivative gain: K_V =25V/rad/s

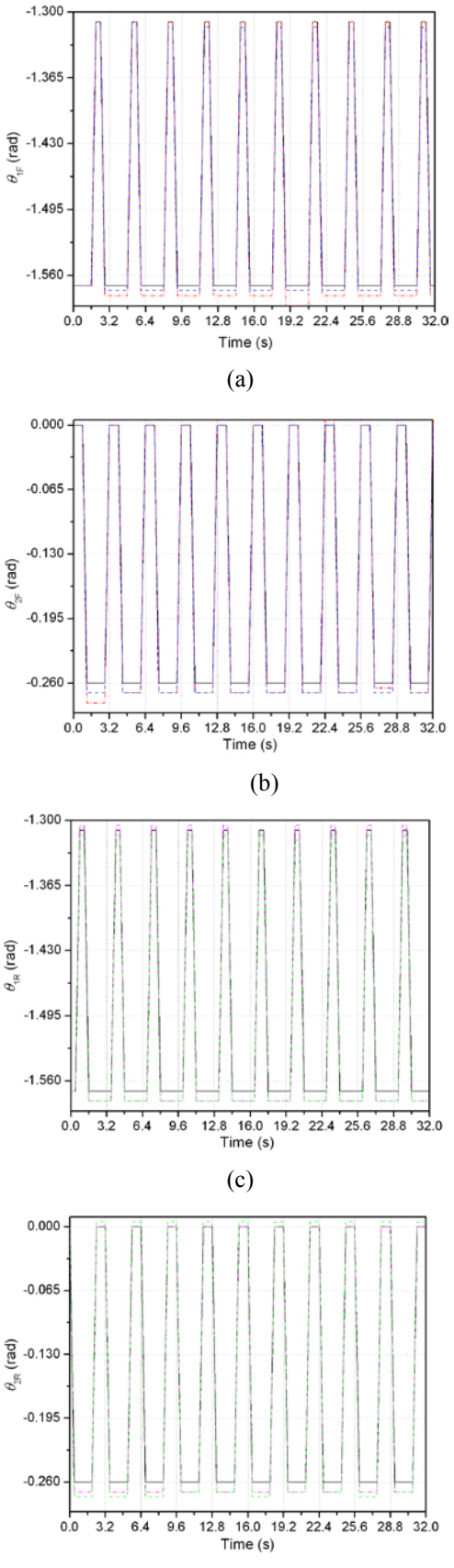

Figure 13: Experimental results: Joint angular displacements (a) θ_{1F} (radians) versus time (s) (b) θ_{2F} (radians) versus time (s) (c) θ_{1R} (radians) versus time (s) (d) θ_{2R} (radians) versus time (s)

REFERENCES

Bowling A., 2005. Mobility and dynamic performance of legged robots. *Proceedings of IEEE International Conference on Robotics and Automation*, pp. 4100-4107, 18-22 April, Barcelona, Spain.

Craig J. J., (2006), *Introduction to Robotics– Mechanics and Control*, Pearson Education, Inc.

Estremera J. and Gonzalez de Santos P., 2002. Free gaits for quadruped robots over irregular terrain. *The International Journal of Robotics Research*, 21, 115-130.

Estremera J. and Waldron K. J., 2006. Leg thrust control for stabilization of dynamic gaits in a quadruped robot. *Proceedings of ROMANSY*, pp. 213-220, June 20-22, Warsaw, Poland.

Furusho J., Sano A., Sakaguchi M., and Koizumi E., 1995. Realization of bounce gait in a quadruped robot with articulate joint type legs. *Proceedings of IEEE International Conference on Robotics and Automation*, pp. 697-702.

Garcia E., Galvez J. A. and Gonzalez de Santos P., 2003. On finding the relevant dynamics for model based controlling walking robots. *Journal of Intelligent and Robotic Systems*, 37(4), 375-398.

Gonzalez De Santos P., Jimenez M. A., 1995. Path tracking with quadruped walking machines using discontinuous gaits. *Computers and Electrical Engineering*, 21(6), 383-396.

Hartikainen K. K., Halme A. J., Lehtinen H. and Koskinen K.O., 1992. MECANT I: A six legged

walking machine for research purposes in outdoor environment. *Proceedings of IEEE International Conference on Robotics and Automation*, pp. 157-163. 12-14 May, Nice, France.

Inagaki S., Yuasa H., Suzuki T. and Arai T., 2006. Wave CPG model for autonomous decentralized multi-legged robot: gait generation and walking speed control", *Robotics and Autonomous Systems*, 54(2), 118-126.

Kurazume R., Yoneda K., and Hirose S., 2001. Feedforward and feedback dynamic trot gait control for a quadruped walking vehicle. *Proceedings of IEEE International Conference on Robotics and Automation*, Vol. 3, pp. 3172-3180, 21-26 May, Seoul, Korea.

Lasa Martin de and Buehler M., 2000. Dynamic compliant walking of a quadruped robot: preliminary experiments. *Proceedings of 3rd Int. Conf. on Climbing and Walking Robots*, 2-4 October, Madrid, Spain.

Mukherjee A., Karmarkar R. and Samantray, (2006). *Bondgraph in modeling simulation and fault identification*, New Delhi, I. K. International Publishing House Pvt. Ltd.

Mukherjee A., 2006. Users Manual of SYMBOLS Shakti, http://www.htcinfo.com/, High-Tech Consultants, S.T.E.P., Indian Institute of Technology, Kharagpur.

Waldron K. and McGhee R., 1986. The adaptive suspension vehicle. *Control Systems Magazine, IEEE*, 6(6), 7-12.

Wyffels, F., D'Haene, M., Waegeman, T., Caluwaerts, K., Nunes, C., Schrauwen, B., 2010. Realization of a passive compliant robot dog. *3rd IEEE International Conference RAS & EMBS on Biomedical Robotics and Biomechatronics* (*BioRob*), pp. 882-886, 26-29 September, Tokyo, Japan.

Yoneda K. and Hirose S., 1992. Dynamic and static fusion gait of quadruped walking vehicle on winding path. *Proceedings of IEEE International Conference on Robotics and Automation*, pp. 143-148, Nice, France.

Zhang C. D. and Song S. M., 1993. A study of the stability of generalized wave gaits. *Mathematical Biosciences*, 115(1), 1-32.